

SUGRA DARK MATTER*

KEITH A. OLIVE

*William I. Fine Theoretical Physics Institute, School of Physics and Astronomy,
 University of Minnesota, Minneapolis, MN 55455 USA
 E-mail: olive@umn.edu*

I review the phenomenological and cosmological constraints on the parameter space associated with the Constrained Minimal Supersymmetric Standard Model (CMSSM). The effect of the recent WMAP determination of the cold dark matter density will be discussed. A very constrained model (based on minimal supergravity relations between the bi- and tri-linear supersymmetry breaking mass terms) will be outlined.

1 Introduction

It is well known that supersymmetric models with conserved R -parity contain one new stable particle which is a candidate for cold dark matter (CDM)¹. There are very strong constraints, however, forbidding the existence of stable or long lived particles which are not color and electrically neutral. Strong and electromagnetically interacting LSPs would become bound with normal matter forming anomalously heavy isotopes. Indeed, there are very strong upper limits on the abundances, relative to hydrogen, of nuclear isotopes², $n/n_H \lesssim 10^{-15}$ to 10^{-29} for $1 \text{ GeV} \lesssim m \lesssim 1 \text{ TeV}$. There are relatively few supersymmetric candidates which are not colored and are electrically neutral. The sneutrino^{3,4} is one possibility, but in the MSSM, it has been excluded as a dark matter candidate by direct⁵ and indirect⁶ searches. Another possibility is the gravitino which is probably the most difficult to exclude. I will concentrate on the remaining possibility in the MSSM, namely the neutralinos.

There are four neutralinos, each of which is a linear combination of the $R = -1$, neutral fermions¹: the wino \tilde{W}^3 , the partner of the 3rd component of the $SU(2)_L$ gauge boson; the bino, \tilde{B} , the partner of the $U(1)_Y$ gauge boson; and the two neutral Higgsinos, \tilde{H}_1 and \tilde{H}_2 . In general, neutralinos can be expressed as a linear combination

$$\chi = \alpha \tilde{B} + \beta \tilde{W}^3 + \gamma \tilde{H}_1 + \delta \tilde{H}_2 \quad (1)$$

The solution for the coefficients α, β, γ and δ for neutralinos that make up the

*SUMMARY OF TALK GIVEN AT THE INTERNATIONAL CONFERENCE 20 YEARS OF SUGRA AND SEARCH FOR SUSY AND UNIFICATION (SUGRA20), NORTHEASTERN UNIVERSITY, BOSTON MA, MARCH 2003.

LSP can be found by diagonalizing the mass matrix

$$(\tilde{W}^3, \tilde{B}, \tilde{H}_1^0, \tilde{H}_2^0) \begin{pmatrix} M_2 & 0 & \frac{-g_2 v_1}{\sqrt{2}} & \frac{g_2 v_2}{\sqrt{2}} \\ 0 & M_1 & \frac{g_1 v_1}{\sqrt{2}} & \frac{-g_1 v_2}{\sqrt{2}} \\ \frac{-g_2 v_1}{\sqrt{2}} & \frac{g_1 v_1}{\sqrt{2}} & 0 & -\mu \\ \frac{g_2 v_2}{\sqrt{2}} & \frac{-g_1 v_2}{\sqrt{2}} & -\mu & 0 \end{pmatrix} \begin{pmatrix} \tilde{W}^3 \\ \tilde{B} \\ \tilde{H}_1^0 \\ \tilde{H}_2^0 \end{pmatrix} \quad (2)$$

where $M_1(M_2)$ are the soft supersymmetry breaking U(1) (SU(2)) gaugino mass terms. μ is the supersymmetric Higgs mixing mass parameter and since there are two Higgs doublets in the MSSM, there are two vacuum expectation values, v_1 and v_2 . One combination of these is related to the Z mass, and therefore is not a free parameter, while the other combination, the ratio of the two vevs, $\tan\beta$, is free.

The most general version of the MSSM, despite its minimality in particles and interactions contains well over a hundred new parameters. The study of such a model would be untenable were it not for some (well motivated) assumptions. These have to do with the parameters associated with supersymmetry breaking. It is often assumed that, at some unification scale, all of the gaugino masses receive a common mass, $m_{1/2}$. The gaugino masses at the weak scale are determined by running a set of renormalization group equations. Similarly, one often assumes that all scalars receive a common mass, m_0 , at the GUT scale (though one may wish to make an exception for the Higgs soft masses). These too are run down to the weak scale. The remaining supersymmetry breaking parameters are the trilinear mass terms, A_0 , which I will also assume are unified at the GUT scale, and the bilinear mass term B . There are, in addition, two physical CP violating phases which will not be considered here.

The natural boundary conditions at the GUT scale for the MSSM would include μ , the two soft Higgs masses (m_1 and m_2) and B in addition to $m_{1/2}$, m_0 , and A_0 . In this case, upon running the RGEs down to a low energy scale and minimizing the Higgs potential, one would predict the values of M_Z , $\tan\beta$, and the Higgs pseudoscalar mass, m_A (in addition to all of the sparticle masses). Since M_Z is known, it is more useful to analyze supersymmetric models where M_Z is input rather than output. It is also common to treat $\tan\beta$ as an input parameter. This can be done at the expense of shifting μ (up to a sign) and B from inputs to outputs. When the supersymmetry breaking Higgs soft masses are also unified at the GUT scale (and take the common value m_0), the model is often referred to as the constrained MSSM or CMSSM. Once these parameters are set, the entire spectrum of sparticle masses at the weak scale can be calculated.

2 Constraints

2.1 The Relic Density

The relic abundance of LSP's is determined by solving the Boltzmann equation for the LSP number density in an expanding Universe. The technique⁷ used is similar to that for computing the relic abundance of massive neutrinos⁸. The relic density depends on additional parameters in the MSSM beyond $m_{1/2}$, μ , and $\tan\beta$. These include the sfermion masses, $m_{\tilde{f}}$, as well as m_A , all derived from m_0 , A_0 , and $m_{1/2}$. To determine the relic density it is necessary to obtain the general annihilation cross-section for neutralinos. In much of the parameter space of interest, the LSP is a bino and the annihilation proceeds mainly through sfermion exchange. Because of the p-wave suppression associated with Majorana fermions, the s-wave part of the annihilation cross-section is suppressed by the outgoing fermion masses. This means that it is necessary to expand the cross-section to include p-wave corrections which can be expressed as a term proportional to the temperature if neutralinos are in equilibrium. The partial wave expansion results in a very good approximation to the relic density except near s-channel annihilation poles, thresholds and in regions where the LSP is nearly degenerate with the next lightest supersymmetric particle⁹, where a more accurate treatment is necessary.

The preferred range of the relic LSP density has always been restricted to a relatively narrow range $0.1 < \Omega_{\text{CDM}} h^2 < 0.3$, where values much smaller than the lower bound are disfavoured by analyses of structure formation in the CDM framework and the upper limit assumes only that the age of the Universe is > 12 Gyr. However, one should note that the LSP may not constitute all the CDM, in which case Ω_{LSP} could be reduced below this value. This range has, however, been altered significantly by the recent improved determination of the allowable range of the cold dark matter density obtained by combining WMAP and other cosmological data: $0.094 < \Omega_{\text{CDM}} < 0.129$ at the 2- σ level¹⁰.

2.2 Accelerator Bounds

The most relevant constraints on the supersymmetric parameter space are: $m_{\chi^\pm} > 104$ GeV¹¹, $m_{\tilde{e}} > 99$ GeV¹² and $m_h > 114$ GeV¹³. The former two constrain $m_{1/2}$ and m_0 directly via the sparticle masses, and the latter indirectly via the sensitivity of radiative corrections to the Higgs mass to the sparticle masses, principally $m_{\tilde{t}, \tilde{b}}$. The latest version of **FeynHiggs**¹⁴ is used for the calculation of m_h . The Higgs limit imposes important constraints principally on $m_{1/2}$ particularly at low $\tan\beta$. Another constraint is the requirement that the branching ratio for $b \rightarrow s\gamma$ is consistent with the experimental measurements¹⁵. These measurements agree with the Standard Model, and therefore provide bounds on MSSM particles, such as the chargino

and charged Higgs masses, in particular. Typically, the $b \rightarrow s\gamma$ constraint is more important for $\mu < 0$, but it is also relevant for $\mu > 0$, particularly when $\tan\beta$ is large. The constraint imposed by measurements of $b \rightarrow s\gamma$ also excludes small values of $m_{1/2}$.

Finally, there are regions of the $(m_{1/2}, m_0)$ plane that are favoured by the BNL measurement¹⁶ of $g_\mu - 2$ at the 2- σ level, corresponding to a deviation of $(33.9 \pm 11.2) \times 10^{-10}$ from the Standard Model calculation¹⁷ using e^+e^- data. One should be however aware that this constraint is still under discussion and it will not be used to constrain $\tan\beta$. All the $\mu > 0$ planes would be consistent with $g_\mu - 2$ at the 3- σ level, whereas $\mu < 0$ is disfavoured even if one takes a relaxed view of the $g_\mu - 2$ constraint.

3 Results for the $m_{1/2} - m_0$ Plane Before and After WMAP

As noted earlier, the spectrum for a given model in the CMSSM is determined by the parameter set $m_{1/2}, m_0, \tan\beta, A_0$, and the sign of μ . For now, I will assume that $A_0 = 0$. Then, for a given value of $\tan\beta$ and $\text{sgn}(\mu)$, the resulting constraints can be displayed on the $m_{1/2} - m_0$ plane. Let us first consider the region of parameter space with relatively low values of $m_{1/2}$ and m_0 , i.e. the ‘bulk’ region in the CMSSM for $\tan\beta = 10$ and $\mu > 0$ shown in Fig. 1¹⁸. The light shaded region corresponds to $0.1 < \Omega_\chi h^2 < 0.3$. The dark shaded region has $m_{\tilde{\tau}_1} < m_\chi$ and is excluded. The light dashed contours indicate the corresponding region in $\Omega_\chi h^2$ if one ignores the effect of coannihilations. Neglecting coannihilations, one would find an upper bound of ~ 450 GeV on $m_{1/2}$, corresponding to an upper bound of roughly 200 GeV on $m_{\tilde{B}}$.

Coannihilations are important when there are several particle species i , with different masses, and each with its own number density n_i and equilibrium number density $n_{0,i}$. In this case inclusion of coannihilations is required because of the degeneracy of χ and $\tilde{\tau}_1$. The effect of coannihilations is to create an allowed band about 25-50 GeV wide in m_0 for $m_{1/2} \lesssim 1400$ GeV, which tracks above the $m_{\tilde{\tau}_1} = m_\chi$ contour^{18,19}.

A larger view of the $\tan\beta = 10$ parameter plane is shown in the left panel of Fig. 2^{18,20,21,22}. Included here are the phenomenological constraints discussed above. As one can see, the region preferred by $g - 2$ overlaps very nicely with the ‘bulk’ region for $\tan\beta = 10$ and $\mu > 0$. In the second panel of Fig. 2, we see the effect of imposing the WMAP range on the neutralino density^{23,24}. We see immediately that (i) the cosmological regions are generally much narrower, and (ii) the ‘bulk’ regions at small $m_{1/2}$ and m_0 have almost disappeared, in particular when the laboratory constraints are imposed. Looking more closely at the coannihilation regions, we see that (iii) they are significantly truncated as well as becoming much narrower, since the reduced upper bound on $\Omega_\chi h^2$ moves the tip where $m_\chi = m_{\tilde{\tau}}$ to smaller $m_{1/2}$ so that the upper limit is now $m_{1/2} \lesssim 950$ GeV or $m_\chi \lesssim 400$ GeV.

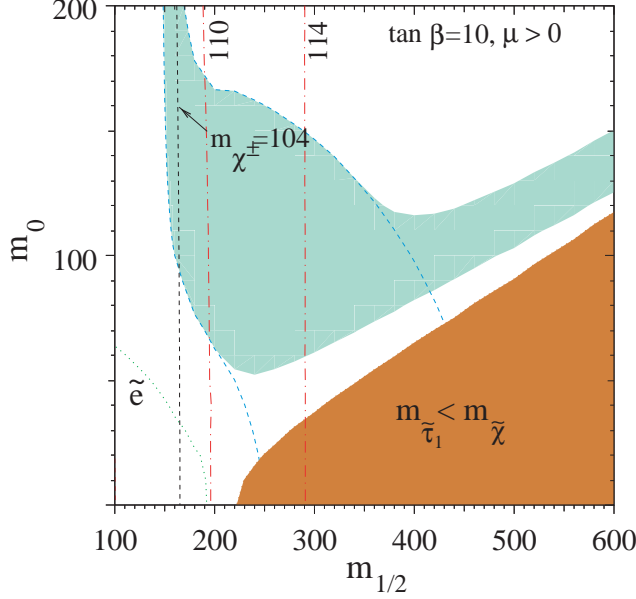


Figure 1. The light-shaded ‘bulk’ area is the cosmologically preferred region with $0.1 \leq \Omega_\chi h^2 \leq 0.3$. The light dashed lines show the location of the cosmologically preferred region if one ignores coannihilations with the light sleptons. In the dark shaded region in the bottom right, the LSP is the $\tilde{\tau}_1$, leading to an unacceptable abundance of charged dark matter. Also shown is the isomass contour $m_{\chi^\pm} = 104$ GeV and $m_h = 110, 114$ GeV, as well as an indication of the slepton bound from LEP.

Another mechanism for extending the allowed CMSSM region to large m_χ is rapid annihilation via a direct-channel pole when $m_\chi \sim \frac{1}{2}m_A$ ^{25,21}. Since the heavy scalar and pseudoscalar Higgs masses decrease as $\tan\beta$ increases, eventually $2m_\chi \simeq m_A$ yielding a ‘funnel’ extending to large $m_{1/2}$ and m_0 at large $\tan\beta$, as seen in Fig. 3. The difficulty and necessary care involved in calculations at large $\tan\beta$ were previously discussed²¹. For related CMSSM calculations see²⁶.

In the second panel of Fig. 3, we see the effect of imposing the WMAP range on the neutralino density²³. We see rapid-annihilation funnels that are also narrower and extend to lower $m_{1/2}$ and m_0 than previously. They weaken significantly the upper bound on m_χ for $\tan\beta \gtrsim 50$ for $\mu > 0$.

Shown in Fig. 4 are the wmap lines²³ of the $(m_{1/2}, m_0)$ plane allowed by the new cosmological constraint $0.094 < \Omega_\chi h^2 < 0.129$ and the laboratory constraints listed above, for $\mu > 0$ and values of $\tan\beta$ from 5 to 55, in steps $\Delta(\tan\beta) = 5$. We notice immediately that the strips are considerably narrower than the spacing between them, though any intermediate point in

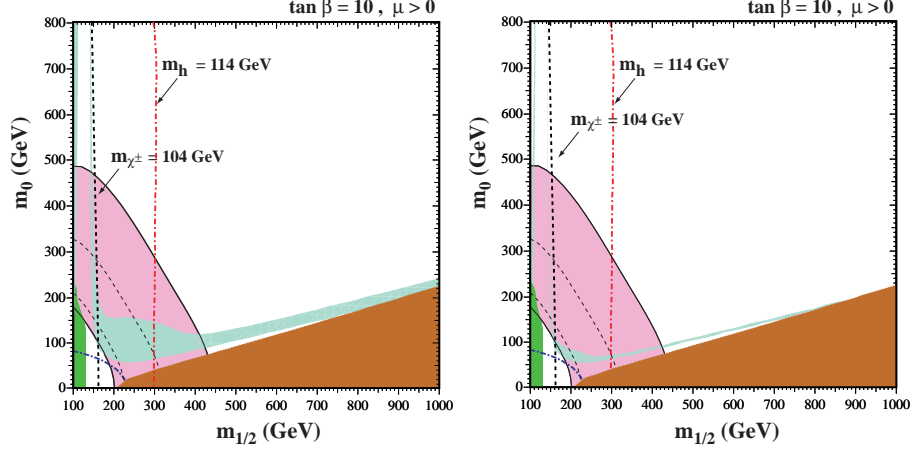


Figure 2. The $(m_{1/2}, m_0)$ planes for (a) $\tan \beta = 10$ and $\mu > 0$, assuming $A_0 = 0$, $m_t = 175$ GeV and $m_b(m_b)_{\overline{MS}}^{SM} = 4.25$ GeV. The near-vertical (red) dot-dashed lines are the contours $m_h = 114$ GeV as calculated using `FeynHiggs` ¹⁴, and the near-vertical (black) dashed line is the contour $m_{\chi^\pm} = 104$ GeV. Also shown by the dot-dashed curve in the lower left is the corner excluded by the LEP bound of $m_{\tilde{e}} > 99$ GeV. The medium (dark green) shaded region is excluded by $b \rightarrow s\gamma$, and the light (turquoise) shaded area is the cosmologically preferred regions with $0.1 \leq \Omega_\chi h^2 \leq 0.3$. In the dark (brick red) shaded region, the LSP is the charged $\tilde{\tau}_1$. The region allowed by the E821 measurement of a_μ at the 2- σ level, is shaded (pink) and bounded by solid black lines, with dashed lines indicating the 1- σ ranges. In (b), the relic density is restricted to the range $0.094 < \Omega_\chi h^2 < 0.129$.

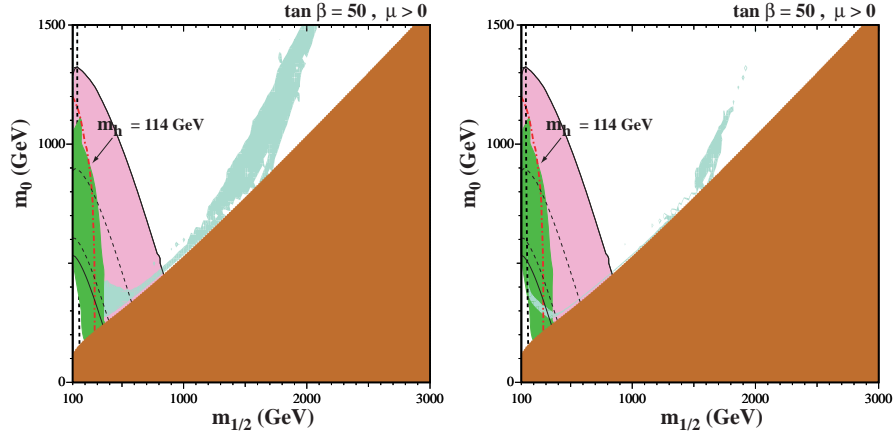


Figure 3. As in Fig. 2 for $\tan \beta = 50$ and $\mu > 0$

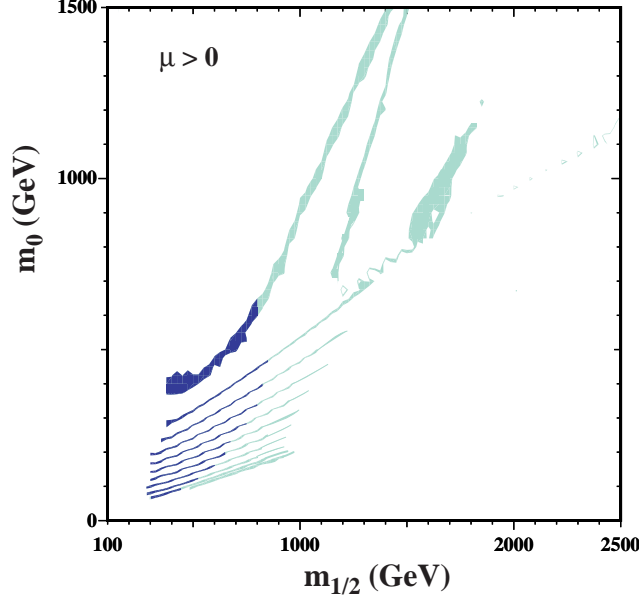


Figure 4. The strips display the regions of the $(m_{1/2}, m_0)$ plane that are compatible with $0.094 < \Omega_\chi h^2 < 0.129$ and the laboratory constraints for $\mu > 0$ and $\tan \beta = 5, 10, 15, 20, 25, 30, 35, 40, 45, 50, 55$. The parts of the strips compatible with $g_\mu - 2$ at the $2\text{-}\sigma$ level have darker shading.

the $(m_{1/2}, m_0)$ plane would be compatible with some intermediate value of $\tan \beta$. The right (left) ends of the strips correspond to the maximal (minimal) allowed values of $m_{1/2}$ and hence m_χ . The lower bounds on $m_{1/2}$ are due to the Higgs mass constraint for $\tan \beta \leq 23$, but are determined by the $b \rightarrow s\gamma$ constraint for higher values of $\tan \beta$. The upper bound on $m_{1/2}$ for $\tan \beta \gtrsim 50$ is clearly weaker, because of the rapid-annihilation regions.

4 Using SUGRA to constrain the CMSSM

While the CMSSM models described above are certainly mSUGRA inspired, minimal supergravity models can be argued to be still more predictive or constrained. Let us begin by assuming that supersymmetry is broken in a hidden sector so that the superpotential can be written as a sum of two terms, $W = F(\phi) + g(\zeta)$, where ϕ represents all observable fields and ζ all hidden sector fields. Then the scalar potential in an $N = 1$ supergravity theory with minimal Kähler potential $K(\phi, \zeta) = \phi\phi^* + \zeta\zeta^* + \ln|W|^2$, can be written as²⁷

$$V = e^{(|\zeta|^2 + |\phi|^2)} \left[\left| \frac{\partial g}{\partial \zeta} + \zeta^* (g(\zeta) + F(\phi)) \right|^2 \right]$$

$$+ \left| \frac{\partial F}{\partial \phi} + \phi^* (g(\zeta) + F(\phi)) \right|^2 - 3 |g(\zeta) + F(\phi)|^2 \right]. \quad (3)$$

We furthermore must choose $g(\zeta)$ such that when ζ picks up a vacuum expectation value, supersymmetry is broken. When the potential is expanded and terms inversely proportional to Planck mass are dropped, one finds^{28,29} 1) scalar mass universality with $m_0 = \langle g \rangle$; 2) trilinear mass universality with $A_0 = \langle dg/d\zeta \rangle \langle \zeta \rangle + \langle g \rangle \langle \zeta \rangle^2$; and 3) $B_0 = A_0 - m_0$.

In fact, one of the primary motivations for the CMSSM, and for scalar mass universality in particular, comes from the simplest model for local supersymmetry breaking³⁰, which involves just one additional chiral multiplet ζ with a superpotential of the form

$$g(\zeta) = \nu(\zeta + \beta) \quad (4)$$

with $|\beta| = 2 - \sqrt{3}$, ensuring that the cosmological constant $\Lambda = 0$. After inserting the vev for ζ , $\langle \zeta \rangle = \sqrt{3} - 1$. The scalar potential in this model takes the form³¹:

$$\begin{aligned} V &= e^{(4-2\sqrt{3})} \left[|\nu + (\sqrt{3} - 1)(\nu + F(\phi))|^2 \right. \\ &\quad \left. + \left| \frac{\partial F}{\partial \phi} + \phi^* (\nu + F(\phi)) \right|^2 - 3 |\nu + F(\phi)|^2 \right] \\ &= e^{(4-2\sqrt{3})} \left| \frac{\partial F}{\partial \phi} \right|^2 \\ &\quad + m_{3/2} e^{(2-\sqrt{3})} \left(\phi \frac{\partial F}{\partial \phi} - \sqrt{3} F + h.c. \right) + m_{3/2}^2 \phi \phi^*, \end{aligned} \quad (5)$$

where the gravitino mass is given by $m_{3/2} = e^{2-\sqrt{3}} \nu$.

First, up to an overall rescaling of the superpotential, $F \rightarrow e^{\sqrt{3}-2} F$, the first term is the ordinary F -term part of the scalar potential of global supersymmetry. The next term, which is proportional to $m_{3/2}$, provides universal trilinear soft supersymmetry-breaking terms $A = (3 - \sqrt{3})m_{3/2}$ and bilinear soft supersymmetry-breaking terms $B = (2 - \sqrt{3})m_{3/2}$, i.e., a special case of the general relation above between B and A . Finally, the last term represents a universal scalar mass of the type advocated in the CMSSM, with $m_0^2 = m_{3/2}^2$, since the cosmological constant Λ vanishes in this model, by construction.

Given a relation between B_0 and A_0 , we can no longer use the standard CMSSM boundary conditions, in which $m_{1/2}$, m_0 , A_0 , $\tan \beta$, and $\text{sgn}(\mu)$ are input at the GUT scale with μ and B determined by the electroweak symmetry breaking condition. Now, one is forced to input B_0 and instead $\tan \beta$ is calculated from the minimization of the Higgs potential³². It should be stressed that this type of model is one that truly originates from minimal supergravity.

In Fig. 5, the contours of $\tan \beta$ (solid blue lines) in the $(m_{1/2}, m_0)$ planes for two values of $\hat{A} = A_0/m_0$, $\hat{B} = B_0/m_0 = \hat{A} - 1$ and the sign of μ are

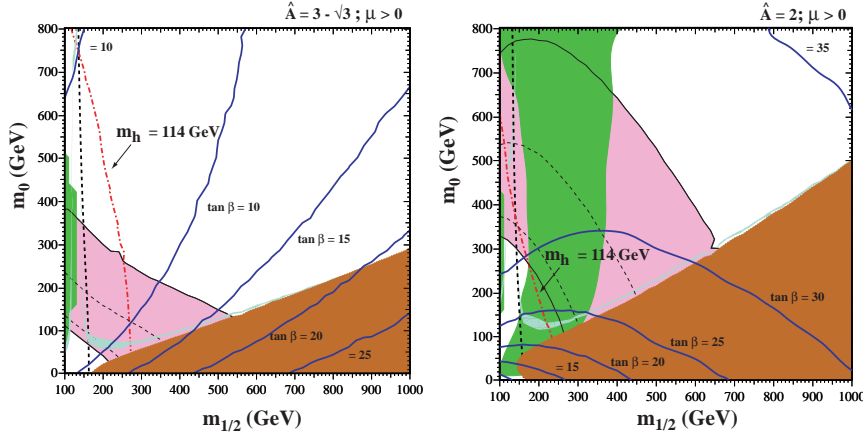


Figure 5. Examples of $(m_{1/2}, m_0)$ planes with contours of $\tan \beta$ superposed, for $\mu > 0$ and (a) the simplest Polonyi model with $\hat{A} = 3 - \sqrt{3}$, $\hat{B} = \hat{A} - 1$ and (b) $\hat{A} = 2.0$, $\hat{B} = \hat{A} - 1$. In each panel, we show the regions excluded by the LEP lower limits on MSSM particles, those ruled out by $b \rightarrow s\gamma$ decay¹⁵ (medium green shading), and those excluded because the LSP would be charged (dark red shading). The region favoured by the WMAP range $\Omega_{CDM}h^2 = 0.1126^{+0.0081}_{-0.0091}$ has light turquoise shading. The region suggested by $g_\mu - 2$ is medium (pink) shaded.

displayed³². Also shown are the contours where $m_{\chi^\pm} > 104$ GeV (near-vertical black dashed lines) and $m_h > 114$ GeV (diagonal red dash-dotted lines). The excluded regions where $m_\chi > m_{\tilde{\tau}_1}$ have dark (red) shading, those excluded by $b \rightarrow s\gamma$ have medium (green) shading, and those where the relic density of neutralinos lies within the WMAP range $0.094 \leq \Omega_\chi h^2 \leq 0.129$ have light (turquoise) shading. Finally, the regions favoured by $g_\mu - 2$ at the 2- σ level are medium (pink) shaded.

In panel (a) of Fig. 5, we see that the Higgs constraint combined with the relic density requires $\tan \beta \gtrsim 11$, whilst the relic density also enforces $\tan \beta \lesssim 20$. For a given point in the $m_{1/2} - m_0$ plane, the calculated value of $\tan \beta$ increases as \hat{A} increases. This is seen in panel (b) of Fig. 5, when $\hat{A} = 2.0$, close to its maximal value for $\mu > 0$, the $\tan \beta$ contours turn over towards smaller $m_{1/2}$, and only relatively large values $25 \lesssim \tan \beta \lesssim 35$ are allowed by the $b \rightarrow s\gamma$ and $\Omega_{CDM}h^2$ constraints, respectively. For any given value of \hat{A} , there is only a relatively narrow range allowed for $\tan \beta$.

At higher values of \hat{A} (and high $\tan \beta$), the off-diagonal elements in the squark mass matrix become large at large m_0 . Therefore, we find no solutions which are phenomenologically viable above $\hat{A} \simeq 2.5$. This is because the regions where the LSP is the $\tilde{\tau}$ or the \tilde{t} close off the parameter space. In fact, this feature is generic in the CMSSM as shown in Fig. 3 of²⁰. This effect is

more severe at large $\tan\beta$, which further compounds the difficulty in going to large values of \hat{A} in the type of models discussed here. At very low values of \hat{A} ($\lesssim -1.9$), there are no viable solutions due to the competition between the Higgs mass bound and the relic density. At low \hat{A} , solutions give low values of $\tan\beta$ which in turn give low Higgs masses unless $m_{1/2}$ is very large. For $\hat{A} < -1.9$, $m_{1/2}$ is pushed passed the endpoint of the coannihilation region.

In addition, we note the absence of the funnel regions. This is due to the relatively small values of $\tan\beta$ allowed in the class of models considered here: we recall that the funnel region appears only for large $\tan\beta \gtrsim 45$ for $\mu > 0$ and $\tan\beta \gtrsim 30$ for $\mu < 0$ in the CMSSM.

Rather than further constrain the CMSSM as described above, one can generalize the CMSSM case to include non-universal Higgs masses^{33,22} (NUHM), in which case the input parameters include μ and m_A , in addition to the standard CMSSM inputs. In this case, the two soft Higgs masses, m_1, m_2 are no longer set equal to m_0 and are calculated from the electroweak symmetry breaking conditions. The NUHM parameter space was recently analyzed²² and a sample of the results were reviewed in³⁴.

Acknowledgments

This work was supported in part by DOE grant DE-FG02-94ER-40823 at the University of Minnesota.

References

1. J. Ellis, J.S. Hagelin, D.V. Nanopoulos, K.A. Olive and M. Srednicki, *Nucl. Phys.* **B238**, 453 (1984);
see also H. Goldberg, *Phys. Rev. Lett.* **50**, 1419 (1983).
2. J. Rich, M. Spiro and J. Lloyd-Owen, *Phys.Rep.* **151**, 239 (1987);
P.F. Smith, *Contemp.Phys.* **29**, 159 (1998);
T.K. Hemmick et al., *Phys.Rev.* **D41**, 2074 (1990). T. Yanagata, Y. Takamori, and H. Utsunomiya, *Phys.Rev.* **D47**, 1231 (1993).
3. L.E. Ibanez, *Phys. Lett.* **137B**, 160 (1984);
J. Hagelin, G.L. Kane, and S. Raby, *Nucl., Phys.* **B241**, 638 (1984).
4. T. Falk, K. A. Olive and M. Srednicki, *Phys. Lett. B* **339**, 248 (1994) [[arXiv:hep-ph/9409270](#)].
5. S. Ahlen, et. al., *Phys. Lett.* **B195**, 603 (1987);
D.D. Caldwell, et. al., *Phys. Rev. Lett.* **61**, 510 (1988);
M. Beck et al., *Phys. Lett.* **B336** 141 (1994).
6. see e.g. K.A. Olive and M. Srednicki, *Phys. Lett.* **205B**, 553 (1988);
N. Sato et al. *Phys.Rev.* **D44**, 2220 (1991).
7. R. Watkins, M. Srednicki and K.A. Olive, *Nucl. Phys.* **B310**, 693 (1988).
8. P. Hut, *Phys. Lett.* **69B**, 85 (1977);

- B.W. Lee and S. Weinberg, *Phys. Rev. Lett.* **39**, 165 (1977).
9. K. Griest and D. Seckel, *Phys.Rev.* **D43**, 3191 (1991).
10. C. L. Bennett *et al.*, arXiv:astro-ph/0302207; D. N. Spergel *et al.*, arXiv:astro-ph/0302209; H. V. Peiris *et al.*, arXiv:astro-ph/0302225.
11. Joint LEP 2 Supersymmetry Working Group, *Combined LEP Chargino Results, up to 208 GeV*,
http://lepsusy.web.cern.ch/lepsusy/www/inos_moriond01/charginos_pub.html.
12. Joint LEP 2 Supersymmetry Working Group, *Combined LEP Selectron/Smuon/Stau Results, 183-208 GeV*,
http://lepsusy.web.cern.ch/lepsusy/www/sleptons_summer02/slep_2002.html.
13. LEP Higgs Working Group for Higgs boson searches, OPAL Collaboration, ALEPH Collaboration, DELPHI Collaboration and L3 Collaboration, *Search for the Standard Model Higgs Boson at LEP*, CERN-EP/2003-011, available from
<http://lephiggs.web.cern.ch/LEPHIGGS/papers/index.html>.
14. S. Heinemeyer, W. Hollik and G. Weiglein, *Comput. Phys. Commun.* **124** (2000) 76 [arXiv:hep-ph/9812320]; S. Heinemeyer, W. Hollik and G. Weiglein, *Eur. Phys. J. C* **9** (1999) 343 [arXiv:hep-ph/9812472].
15. M.S. Alam *et al.*, [CLEO Collaboration], *Phys. Rev. Lett.* **74** (1995) 2885 as updated in S. Ahmed *et al.*, CLEO CONF 99-10; BELLE Collaboration, BELLE-CONF-0003, contribution to the 30th International conference on High-Energy Physics, Osaka, 2000. See also K. Abe *et al.*, [Belle Collaboration], [arXiv:hep-ex/0107065]; L. Lista [BaBar Collaboration], [arXiv:hep-ex/0110010]; C. Degrandi, P. Gambino and G. F. Giudice, *JHEP* **0012** (2000) 009 [arXiv:hep-ph/0009337]; M. Carena, D. Garcia, U. Nierste and C. E. Wagner, *Phys. Lett. B* **499** (2001) 141 [arXiv:hep-ph/0010003]; P. Gambino and M. Misiak, *Nucl. Phys. B* **611** (2001) 338; D. A. Demir and K. A. Olive, *Phys. Rev. D* **65** (2002) 034007 [arXiv:hep-ph/0107329]; T. Hurth, arXiv:hep-ph/0212304.
16. G. W. Bennett *et al.* [Muon g-2 Collaboration], *Phys. Rev. Lett.* **89** (2002) 101804 [Erratum-ibid. **89** (2002) 129903] [arXiv:hep-ex/0208001].
17. M. Davier, S. Eidelman, A. Hocker and Z. Zhang, arXiv:hep-ph/0208177; see also K. Hagiwara, A. D. Martin, D. Nomura and T. Teubner, arXiv:hep-ph/0209187; F. Jegerlehner, unpublished, as reported in M. Krawczyk, arXiv:hep-ph/0208076.
18. J. Ellis, T. Falk, and K.A. Olive, *Phys.Lett.* **B444** (1998) 367 [arXiv:hep-ph/9810360]; J. Ellis, T. Falk, K.A. Olive, and M. Srednicki, *Astr. Part. Phys.* **13** (2000) 181 [Erratum-ibid. **15** (2001) 413] [arXiv:hep-ph/9905481].
19. M. E. Gómez, G. Lazarides and C. Pallis, *Phys.Rev.* **D61** (2000) 123512 [arXiv:hep-ph/9907261]; *Phys.Lett.* **B487** (2000) 313 [arXiv:hep-ph/0004028]; *Nucl. Phys.* **B638** (2002) 165 [arXiv:hep-ph/0203131]; R. Arnowitt, B. Dutta and Y. Santos, *Nucl. Phys.* **B606** (2001) 59; T. Nihei, L. Roszkowski and R. Ruiz de Aus-

- tri, *JHEP* **0207** (2002) 024 [arXiv:hep-ph/0206266]; H. Baer, C. Balazs and A. Belyaev, *JHEP* **0203**, 042 (2002) [arXiv:hep-ph/0202076]; G. Belanger, F. Boudjema, A. Pukhov and A. Semenov, arXiv:hep-ph/0112278.
20. J. R. Ellis, T. Falk, G. Ganis and K. A. Olive, *Phys. Rev. D* **62**, 075010 (2000) [arXiv:hep-ph/0004169].
 21. J. R. Ellis, T. Falk, G. Ganis, K. A. Olive and M. Srednicki, *Phys. Lett. B* **510** (2001) 236 [arXiv:hep-ph/0102098].
 22. J. Ellis, K. Olive and Y. Santoso, *Phys. Lett. B* **539** (2002) 107 [arXiv:hep-ph/0204192].; J. R. Ellis, T. Falk, K. A. Olive and Y. Santoso, *Nucl. Phys. B* **652** (2003) 259 [arXiv:hep-ph/0210205].
 23. J. R. Ellis, K. A. Olive, Y. Santoso and V. C. Spanos, *Phys. Lett. B* **565** (2003) 176 [arXiv:hep-ph/0303043].
 24. H. Baer and C. Balazs, arXiv:hep-ph/0303114. A. B. Lahanas and D. V. Nanopoulos, arXiv:hep-ph/0303130. U. Chattopadhyay, A. Corsetti and P. Nath, arXiv:hep-ph/0303201.
 25. M. Drees and M. M. Nojiri, *Phys. Rev. D* **47** (1993) 376; H. Baer and M. Brhlik, *Phys. Rev. D* **53** (1996) 59; and *Phys. Rev. D* **57** (1998) 567; H. Baer, M. Brhlik, M. A. Diaz, J. Ferrandis, P. Mercadante, P. Quintana and X. Tata, *Phys. Rev. D* **63** (2001) 015007; A. B. Lahanas, D. V. Nanopoulos and V. C. Spanos, *Mod. Phys. Lett. A* **16** (2001) 1229.
 26. A. B. Lahanas, D. V. Nanopoulos and V. C. Spanos, *Phys. Rev. D* **62** (2000) 023515 [arXiv:hep-ph/9909497]; V. Barger and C. Kao, *Phys. Lett. B* **518** (2001) 117 [arXiv:hep-ph/0106189]; L. Roszkowski, R. Ruiz de Austri and T. Nihei, *JHEP* **0108** (2001) 024 [arXiv:hep-ph/0106334]; A. Djouadi, M. Drees and J. L. Kneur, *JHEP* **0108** (2001) 055 [arXiv:hep-ph/0107316]; R. Arnowitt and B. Dutta, arXiv:hep-ph/0211417; H. Baer, C. Balazs and A. Belyaev, *JHEP* **0203** (2002) 042 [arXiv:hep-ph/0202076]; T. Kamon, R. Arnowitt, B. Dutta and V. Khotilovich, arXiv:hep-ph/0302249; H. Baer, C. Balazs, A. Belyaev, T. Krupovnickas and X. Tata, arXiv:hep-ph/0304303.
 27. E. Cremmer, B. Julia, J. Scherk, S. Ferrara, L. Girardello and P. Van Nieuwenhuizen, *Phys. Lett. B* **79** (1978) 231; and *Nucl. Phys. B* **147** (1979) 105; E. Cremmer, S. Ferrara, L. Girardello and A. Van Proeyen, *Phys. Lett. B* **116** (1982) 231; and *Nucl. Phys. B* **212** (1983) 413; R. Arnowitt, A.H. Chamseddine and P. Nath, *Phys. Rev. Lett.* **49** (1982) 970; **50** (1983) 232 and *Phys. Lett. B* **121** (1983) 33; J. Bagger and E. Witten, *Phys. Lett. B* **115** (1982) 202 and **118** (1982) 103; J. Bagger, *Nucl. Phys. B* **211** (1983) 302.
 28. For reviews, see: H. P. Nilles, *Phys. Rep.* **110** (1984) 1; A. Brignole, L. E. Ibanez and C. Munoz, arXiv:hep-ph/9707209, published in *Perspectives on supersymmetry*, ed. G. L. Kane, pp. 125-148.
 29. H.-P. Nilles, M. Srednicki and D. Wyler, *Phys. Lett. B* **120** (1983) 345; L.J. Hall, J. Lykken and S. Weinberg, *Phys. Rev. D* **27** (1983) 2359.

30. J. Polonyi, Budapest preprint KFKI-1977-93 (1977).
31. R. Barbieri, S. Ferrara and C.A. Savoy, *Phys. Lett.* **119B** (1982) 343.
32. J. Ellis, K. A. Olive, Y. Santoso and V. C. Spanos, arXiv:hep-ph/0305212.
33. M. Drees, M. M. Nojiri, D. P. Roy and Y. Yamada, *Phys.Rev.* **D56** (1997) 276 [Erratum-ibid. **D64** (1997) 039901] [arXiv:hep-ph/9701219];
M. Drees, Y. G. Kim, M. M. Nojiri, D. Toya, K. Hasuko and
T. Kobayashi, *Phys.Rev.* **D63** (2001) 035008 [arXiv:hep-ph/0007202].
V. Berezhinsky, A. Bottino, J. R. Ellis, N. Fornengo, G. Mignola and
S. Scopel, *Astropart. Phys.* **5** (1996) 1 [arXiv:hep-ph/9508249]; P. Nath
and R. Arnowitt, *Phys.Rev.* **D56** (1997) 2820 [arXiv:hep-ph/9701301];
A. Bottino, F. Donato, N. Fornengo and S. Scopel, *Phys.Rev.* **D63**
(2001) 125003 [arXiv:hep-ph/0010203]; V. Bertin, E. Nezri and J. Orloff,
arXiv:hep-ph/0210034.
34. Y. Santoso, arXiv:hep-ph/0307356.